



Cite this: DOI: 10.1039/d1nj02893f

# The first report of X-ray characterized organosilatrane-based receptors for the electrochemical analysis of Al<sup>3+</sup> ions†

 Gurjaspreet Singh,<sup>a</sup> Sanjay Sharma,<sup>a</sup> Akshpreet Singh,<sup>b</sup> Ranjeet Kaur,<sup>a</sup> Pawan,<sup>a</sup> Mohit,<sup>a</sup> Shweta Rana,<sup>a</sup> Subash Chandra Sahoo<sup>b</sup> and Amarjit Kaur<sup>\*a</sup>

The present work reports for the first time the preparation of aryl-alkyl ether functionalized silatrane for the selective recognition of Al<sup>3+</sup> ions using the cyclic voltammetry technique. The synthesis was achieved through a condensation reaction followed by transesterification methodology to obtain organosilatrane in good yields. The prepared compounds were well characterized by IR, NMR (<sup>1</sup>H and <sup>13</sup>C) and mass spectral analysis and the structure of one of the molecules was further confirmed by X-ray crystallography, which showed a triclinic crystal system with a *P* $\bar{1}$  space group. The electrochemical behaviour was studied by employing square wave voltammetry (SWV) using a gold electrode to investigate the receptor action of the synthesized organosilatrane. A detection limit of 48.9 nM and competitive binding results suggest the significant receptor potential of organosilatrane for the detection of Al<sup>3+</sup> ions. Moreover, the real time application of the prepared sensors was confirmed by the determination of Al<sup>3+</sup> ions in tea leaves.

 Received 13th June 2021,  
 Accepted 23rd July 2021

DOI: 10.1039/d1nj02893f

rsc.li/njc

## Introduction

Organosilatrane refers to the category of hypervalent atrane complexes of silicon having a general formula N-[(CR<sub>1</sub>R<sub>2</sub>)<sub>n</sub>O]<sub>3</sub>-SiR. The molecules contain a tricyclic cage-like structure with a prominent feature of transannular coordinate interactions between their silicon and nitrogen atoms.<sup>1,2</sup> This dative bonding between heteroatoms imparts a pentacoordinated geometry and results in structural stability, some unique chemical properties and architectural beauty.<sup>3</sup> There is increasing interest among chemists for studying these initially called triptych-siloxazolidines due to their widespread applications in the fields of chemosensing, synthesis, catalysis and agriculture, and biological activities.<sup>4,5</sup> Several different types of functionalized silatrane bearing axial substituents like pseudohalogen, organyl, aminoalkyl, organoxy, acyloxy and other groups have been designed and found to have an imperative role as an anti-pilotropic agent, an anti-cancer agent, an anti-tumor agent, a reducing agent and a precursor for preparing porous materials.<sup>4</sup> Furthermore, these are hydrolytically less susceptible than organosilanes, their open chain analogue. The coordination sites in the Schiff base containing silatrane are the

basis for their applications to detect numerous analytes. Moreover, they act as an anti-cancer agent by inhibition of cell proliferation and as an angiotensin-converting enzyme (ACE) and  $\alpha$ -amylase inhibitor.<sup>6,7</sup>

Aluminium, the third most abundant element in the environment, is extensively employed for various human activities such as household works, electronics, construction materials, medical appliances and electricals.<sup>8</sup> The ingestion of this element *via* sources like food additives, deodorants, utensils, *etc.* leads to accumulation in the body that can be the causative agent of various diseases such as encephalopathy, myopathy, Al-related bone diseases, microcytic hypochromic anaemia, dementia, seizures, Alzheimer's disease, motor neuron degeneration and Parkinson's disease.<sup>9-14</sup> The use of Al<sup>3+</sup> ions also has toxic effects on fish, algae, the growth of plants and other aquatic organisms.<sup>15,16</sup> Due to these widespread health hazards of its exposure, there is an urgent requirement to monitor the presence of Al<sup>3+</sup> ions in biological, food and environment samples by designing selective receptors. So, a need to design and prepare selective, portable and sensitive probes for the recognition of aluminium(III) ions arises. Several traditional techniques of spectrophotometry for metal ion recognition have been employed but electrochemical techniques can give reproducible outcomes and are always characterized by their high degree of precision, sensitivity, cost-effectiveness, portability and simplicity.<sup>17-28</sup> The present research undertakes the work of utilizing organosilatrane to analyze the Al<sup>3+</sup> ions using square wave anodic stripping voltammetry (SWASV), which is

<sup>a</sup> Department of Chemistry and Centre of Advanced Studies, Panjab University, Chandigarh, 160014, India. E-mail: gipsingh@pu.ac.in, amarjitk@pu.ac.in

<sup>b</sup> Department of Chemistry, DAV College, Sector-10, Chandigarh 160011, India

† Electronic supplementary information (ESI) available. CCDC 2062598 of 5(c). For ESI and crystallographic data in CIF or other electronic format see DOI: 10.1039/d1nj02893f

the first of this kind. The inclusion of the Schiff base unit into the molecular system enhanced the complexation ability of the sensor and the receptor has also been practically applied to real samples. There are many known recognized probes for the determination of aluminium(III) ions but the investigation in this report has abundant benefits, for example, cost-effectiveness, free from dangerous materials, sensitivity, portability, selectivity, rapid response and simplicity.

## Experimental section

### Materials and methods

4'-Bromomethyl-2-biphenylcarbonitrile (Avra), carboaldehydes (Avra), potassium hydroxide (Avra), triethanol amine (Merck), and amino propyl silane (Aldrich) were purchased and used as received. Inorganic chloride salts of cobalt, copper, aluminium, nickel, zinc, mercury, rubidium, lanthanum, cerium and cadmium were purchased from S.D. Fine Chem Ltd, India. All the solvents used were dried properly according to the standard procedure.<sup>29</sup> All reactions were carried out under a nitrogen gas. Infrared spectra were recorded as neat spectra using a Thermo Scientific NICOLET IS50 spectrophotometer. <sup>1</sup>H (400 MHz) and <sup>13</sup>C (126 MHz) were recorded using a FT NMR spectrometer model Advance-II (Bruker) using dimethylsulphoxide as the reference. The exact mass was recorded using a Q-TOF MASS spectrometer. The compound 5(e) was characterized



Gurjaspreet Singh

*Dr Gurjaspreet Singh is a Professor in the Department of Chemistry at Panjab University, Chandigarh, India. He has more than 20 years of experience in teaching as well as in research. He is highly experienced in organometallics, bio-inorganic, and organotransition chemistry. His research work is primarily based on the Chemistry of Organosilicon Compounds focusing precisely on the design, synthesis, characterization and properties of new organic compounds, especially*

*the biological activity of bonded metals. He has published more than 100 research papers in various internationally peer reviewed journals. He had the privilege of introducing the Click Silylation term in Organosilicon chemistry and using this term, he has published more than 30 papers in Internationally peer reviewed journals. To date, 20 students have completed their doctorate degree under his supervision. Apart from PhD students, to date, he has also acted as a supervisor for MSc students (more than 80) for their dissertation work. He has successfully completed UGC, DST SERB and CSIR major research projects with 60 publications. A lot of his research work has been presented in various conferences and professional meetings. He is a Life Member of Chemical Research Society of India and of the Indian Science Congress Association. He has been reviewing research articles for various international peer reviewed journals.*

by single X-ray crystallography. All electrochemical measurements were carried out using the classical three electrodes electrochemical cell, wherein Ag/AgCl/KCl acts as the reference electrode, a gold electrode as the working electrode and Pt wire as the counter electrode.

### General procedure for the synthesis of organosilanes 4(a-e)

Compounds 3(a-e) were synthesized by reacting 4'-bromomethyl-2-biphenylcarbonitrile (1) and hydroxy-carboaldehydes 2(a-e) as reported in the literature.<sup>30</sup> In a 100 mL two-neck flask, the compounds 3(a-e) (1 mmol) were dissolved in dry toluene followed by the addition of 3-aminopropyltriethoxysilane (1 mmol) under a nitrogen atmosphere. The reaction mixture was stirred and refluxed at 60 °C overnight. The solvent was evaporated under vacuum and after this, dry ether was added to obtain oily solid organosilanes.

**Synthesis of 4'-((2-(((3-(trimethoxysilyl) propyl)imino)methyl)phenoxy)methyl)[1,1'-biphenyl]-2-carbonitrile 4(a).** Yield: 88% and m.p.: 108–110 °C. <sup>1</sup>H NMR (400 MHz, DMSO-*d*<sub>6</sub>) δ 8.63 (s, 1H), 8.38 (s, 1H), 8.07–7.72 (m, 3H), 7.69–7.25 (m, 6H), 7.24–6.68 (m, 2H), 5.23 (OCH<sub>2</sub>, s, 2H), 3.52 (NCH<sub>2</sub>, (OCH<sub>3</sub>)<sub>3</sub>, 11H), 1.65 (propylCCH<sub>2</sub>C, s, 2H), and 0.57 (SiCH<sub>2</sub>, s, 2H). <sup>13</sup>C NMR (101 MHz, DMSO-*d*<sub>6</sub>) δ 160.26, 144.79, 138.11, 133.80, 133.45, 129.99, 129.36, 128.88, 128.73, 128.18, 127.92, 118.48, 114.72, 110.08, 68.85, 62.31, 48.57, 23.72, and 9.98.

**Synthesis of 4'-((2-(((3-(trimethoxysilyl) propyl)imino)methyl)phenoxy)methyl)[1,1'-biphenyl]-2-carbonitrile 4(b).** Yield: 83% and m.p.: 107–109 °C. <sup>1</sup>H NMR (500 MHz, DMSO-*d*<sub>6</sub>) δ 8.22 (s, 1H), 7.92 (s, 1H), 7.75 (s, 1H), 7.64–7.45 (m, 5H), 7.37 (s, 2H), 7.28 (s, 2H), 7.07 (s, 1H), 5.15 (OCH<sub>2</sub>, s, 2H), 3.66 (NCH<sub>2</sub>, (OCH<sub>3</sub>)<sub>3</sub>, 11H), 1.70 (propylCCH<sub>2</sub>C, s, 2H), and 0.59 (SiCH<sub>2</sub>, s, 2H). <sup>13</sup>C NMR (126 MHz, DMSO-*d*<sub>6</sub>) δ 161.01, 158.99, 144.60, 137.71, 134.29, 133.94, 130.50, 129.19, 128.78, 128.65, 128.34, 121.35, 118.99, 117.68, 113.51, 69.23, 63.00, 49.06, 24.53, and 10.18.

**Synthesis of 4'-((2-(((3-(trimethoxysilyl) propyl)imino)methyl)phenoxy)methyl)[1,1'-biphenyl]-2-carbonitrile 4(c).** Yield: 85% and m.p.: 106–108 °C. <sup>1</sup>H NMR (500 MHz, DMSO-*d*<sub>6</sub>) δ 8.41–7.87 (m, 2H), 7.84–7.26 (m, 8H), 7.25–6.81 (m, 3H), 5.22 (OCH<sub>2</sub>, s, 2H), 4.11 (NCH<sub>2</sub>, s, 2H), 3.41 ((OCH<sub>3</sub>)<sub>3</sub>, s, 9H), 1.72 (propylCCH<sub>2</sub>C, s, 2H), and 0.66 (SiCH<sub>2</sub>, s, 2H). <sup>13</sup>C NMR (126 MHz, DMSO-*d*<sub>6</sub>) δ 161.64, 144.43, 137.81, 134.29, 133.92, 129.84, 129.36, 129.23, 128.67, 128.38, 125.78, 118.97, 115.22, 110.58, 69.35, 63.88, 49.06, and 21.50.

**Synthesis of 4'-((2-methoxy-4-(((3-(trimethoxysilyl) propyl)imino)methyl)phenoxy)methyl)[1,1'-biphenyl]-2-carbonitrile 4(d).** Yield: 81% and m.p.: 104–106 °C. <sup>1</sup>H NMR (500 MHz, DMSO-*d*<sub>6</sub>) δ 8.20–8.04 (m, 1H), 7.97–7.84 (m, 1H), 7.73 (t, *J* = 7.6 Hz, 1H), 7.60–7.44 (m, 6H), 7.37–7.30 (m, 1H), 7.22–6.85 (m, 3H), 5.10 (OCH<sub>2</sub>, s, 2H), 3.72 (NCH<sub>2</sub>, t, *J* = 8.6 Hz, 2H), 3.18 ((OCH<sub>3</sub>)<sub>3</sub>, OCH<sub>3</sub>, s, s, 12H), 1.69 (propylCCH<sub>2</sub>C, s, 2H), and 0.63 (SiCH<sub>2</sub>, s, 2H). <sup>13</sup>C NMR (126 MHz, DMSO-*d*<sub>6</sub>) δ 159.64, 158.93, 144.67, 137.79, 134.31, 134.04, 133.93, 130.59, 130.46, 129.36, 129.28, 129.17, 128.67, 128.58, 128.47, 122.52, 119.03, 113.30, 110.61, 69.89, 59.69, 57.62, 50.44, 27.43, and 15.34.

**Synthesis of 4'-((2-ethoxy-4-(((3-(trimethoxysilyl) propyl)imino)methyl)phenoxy)methyl)[1,1'-biphenyl]-2-carbonitrile 4(e).** Yield: 80% and m.p.: 106–108 °C. <sup>1</sup>H NMR (500 MHz, DMSO-*d*<sub>6</sub>) δ 8.08 (s, 1H), 7.94 (s, 1H), 7.75 (s, 1H), 7.56 (s, 6H), 7.36 (s, 2H), 7.16 (s, 1H), 7.05 (s, 1H), 5.15 (OCH<sub>2</sub>, s, 2H), 3.98 (OCH<sub>2</sub>CH<sub>3</sub>, s, 2H), 3.22 (NCH<sub>2</sub>,

(OCH<sub>3</sub>)<sub>3</sub>, s, 11H), 1.72 (propylCCH<sub>2</sub>C, s, 2H), 1.27 (OCH<sub>2</sub>CH<sub>3</sub>, s, 3H), and 0.66 (SiCH<sub>2</sub>, s, 2H). <sup>13</sup>C NMR (126 MHz, DMSO-*d*<sub>6</sub>) δ 161.99, 161.07, 144.56, 137.68, 134.28, 133.89, 130.46, 130.10, 129.17, 128.65, 128.18, 122.52, 118.97, 111.33, 110.57, 69.92, 64.19, 49.06, 24.78, and 15.06.

#### General procedure for the synthesis of organosilatrane 5(a–e)

Organosilanes 4(a–e) (1 mmol) and triethanolamine (1 mmol) were dissolved in dry toluene with a catalytic amount of potassium hydroxide in a two-neck RBF attached with Deanstark under nitrogen gas. The reaction mixture was refluxed at 65 °C overnight and heated up to 80 °C. The solvent was evaporated under vacuum and a sticky solid product was formed.

**Synthesis of 4'-((3-(2,8,9-trioxa-5-aza-1-silabicyclo[3.3.3]undec-1-yl)propyl)imino)methylphenoxy)methyl[1,1'-biphenyl]-2-carbonitrile 5(a).** Yield: 88% and m.p.: 136–138 °C. <sup>1</sup>H NMR (400 MHz, DMSO-*d*<sub>6</sub>) δ 8.53 (s, 1H), 8.21 (s, 1H), 7.86–7.77 (m, 1H), 7.77–7.61 (m, 2H), 7.61–7.35 (m, 5H), 7.28 (td, *J* = 7.9, 7.3, 1.9 Hz, 1H), 7.06 (dd, *J* = 16.8, 8.0 Hz, 1H), 6.87 (t, *J* = 7.5 Hz, 1H), 5.18 (OCH<sub>2</sub>, s, 2H), 3.46–3.42 (O(CH<sub>2</sub>)<sub>2</sub>, m, 6H), 3.27 (NCH<sub>2</sub>, s, 2H), 2.62 (N(CH<sub>2</sub>)<sub>2</sub>, t, *J* = 5.9 Hz, 6H), 1.57–1.35 (propyl CCH<sub>2</sub>C, m, 2H), and 0.02 (SiCH<sub>2</sub>, m, 2H). <sup>13</sup>C NMR (101 MHz, DMSO-*d*<sub>6</sub>) δ 157.71, 155.22, 144.46, 138.10, 137.77, 134.33, 134.02, 132.08, 130.59, 129.36, 128.75, 128.15, 127.25, 125.20, 121.34, 119.02, 113.69, 110.62, 79.68, 69.63, 65.45, 57.67, 27.33, and 15.19. Calculated ESI-TOF-MS (*m/z*): 528 (M + H)<sup>+</sup> and observed mol. wt: 527.

**Synthesis of 4'-((3-(2,8,9-trioxa-5-aza-1-silabicyclo[3.3.3]undec-1-yl)propyl)imino)methylphenoxy)methyl[1,1'-biphenyl]-2-carbonitrile 5(b).** Yield: 88% and m.p.: 134–136 °C. <sup>1</sup>H NMR (500 MHz, DMSO-*d*<sub>6</sub>) δ 8.29 (s, 1H), 8.01 (dt, *J* = 8.9, 4.5 Hz, 1H), 7.86 (tt, *J* = 6.6, 3.3 Hz, 1H), 7.68 (d, *J* = 3.3 Hz, 7H), 7.49 (d, *J* = 1.0 Hz, 1H), 7.45–7.39 (m, 1H), 7.36 (d, *J* = 7.6 Hz, 1H), 7.25–7.14 (m, 1H), 5.29 (OCH<sub>2</sub>, s, 2H), 3.64 (NCH<sub>2</sub>, O(OCH<sub>2</sub>)<sub>2</sub>, t, *J* = 5.8 Hz, 8H), 2.82 (N(CH<sub>2</sub>)<sub>2</sub>, dd, *J* = 7.4, 4.2 Hz, 6H), 1.70–1.63 (propylCCH<sub>2</sub>C, m, 2H), and 0.24–0.17 (SiCH<sub>2</sub>, m, 2H). <sup>13</sup>C NMR (126 MHz, DMSO-*d*<sub>6</sub>) δ 159.95, 159.04, 144.69, 138.09, 137.79, 134.32, 130.59, 129.36, 129.28, 128.73, 128.67, 128.58, 128.47, 125.77, 122.50, 121.37, 119.03, 117.69, 113.24, 110.64, 69.26, 64.94, 59.70, 57.66, 27.44, and 15.31. Calculated ESI-TOF-MS (*m/z*): 528 (M + H)<sup>+</sup> and observed mol. wt: 527.

**Synthesis of 4'-((4-(2,8,9-trioxa-5-aza-1-silabicyclo[3.3.3]undec-1-yl)propyl)imino)methylphenoxy)methyl[1,1'-biphenyl]-2-carbonitrile 5(c).** Yield: 88% and m.p.: 130–134 °C. <sup>1</sup>H NMR (500 MHz, DMSO-*d*<sub>6</sub>) δ 8.17 (s, 1H), 8.06–7.71 (m, 3H), 7.69–7.53 (m, 7H), 7.10 (d, *J* = 8.7 Hz, 2H), 5.23 (OCH<sub>2</sub>, s, 2H), 4.39 (NCH<sub>2</sub>, s, 2H), 3.64–3.51 (O(CH<sub>2</sub>)<sub>2</sub>, m, 6H), 2.54 (N(CH<sub>2</sub>)<sub>2</sub>, dd, *J* = 16.9, 10.8 Hz, 6H), 1.70–1.54 (propylCCH<sub>2</sub>C, s, 2H), and 0.24–0.09 (SiCH<sub>2</sub>, s, 2H). <sup>13</sup>C NMR (126 MHz, DMSO-*d*<sub>6</sub>) δ 160.42, 159.27, 144.66, 137.85, 134.32, 134.01, 130.58, 130.05, 129.75, 129.30, 128.72, 128.48, 119.03, 115.27, 110.64, 69.35, 65.01, 59.71, 57.48, 50.45, 27.47, and 15.34. Calculated ESI-TOF-MS (*m/z*): 528 (M + H)<sup>+</sup> and observed mol. wt: 527.

**Synthesis of 4'-((2-methoxy-4-(((3-(2,8,9-trioxa-5-aza-1-silabicyclo[3.3.3]undec-1-yl)propyl)imino)methyl)phenoxy)methyl[1,1'-biphenyl]-2-carbonitrile 5(d).** Yield: 88% and m.p.: 131–135 °C. <sup>1</sup>H NMR (500 MHz, DMSO-*d*<sub>6</sub>) δ 8.31 (s, 1H), 8.15 (s, 1H), 7.99–7.73 (m, 2H), 7.64–7.54 (m, 5H), 7.40 (d, *J* = 1.8 Hz, 1H), 7.23–7.10 (m, 3H), 5.21 (OCH<sub>2</sub>, s, 2H), 3.82 (NCH<sub>2</sub>, OCH<sub>3</sub>, s, 5H), 3.59 (O(CH<sub>2</sub>)<sub>2</sub>, t, *J* = 5.8 Hz, 6H), 2.55 (N(CH<sub>2</sub>)<sub>2</sub>, t, *J* = 6.1 Hz, 6H), 1.68–1.55 (propylCCH<sub>2</sub>C, s, 2H), and 0.61 (SiCH<sub>2</sub>, s, 2H). <sup>13</sup>C NMR (126 MHz, DMSO-*d*<sub>6</sub>) δ 164.29, 154.47, 149.43, 142.60, 139.05, 138.73, 135.32, 135.10, 134.78, 134.10, 134.02, 133.40, 133.32, 130.51, 127.25, 123.77, 118.01, 115.40, 114.52, 69.70, 64.46, 62.43, 61.98, 55.21, 26.24, and 20.10. Calculated ESI-TOF-MS (*m/z*): 596 (M + K)<sup>+</sup> and observed mol. wt: 557.

**Synthesis of 4'-((2-ethoxy-4-(((3-(2,8,9-trioxa-5-aza-1-silabicyclo[3.3.3]undec-1-yl)propyl)imino)methyl)phenoxy)methyl[1,1'-biphenyl]-2-carbonitrile 5(e).** Yield: 83% and m.p.: 134–138 °C. <sup>1</sup>H NMR (500 MHz, DMSO-*d*<sub>6</sub>) δ 8.31 (s, 1H), 8.15 (s, 1H), 7.99–7.73 (m, 2H), 7.64–7.54 (m, 5H), 7.40 (d, *J* = 1.8 Hz, 1H), 7.23–7.10 (m, 3H), 5.21 (OCH<sub>2</sub>, s, 2H), 3.82 (NCH<sub>2</sub>, s, 2H), 3.59 (O(CH<sub>2</sub>)<sub>2</sub>, t, *J* = 5.8 Hz, 6H), 2.55 (N(CH<sub>2</sub>)<sub>2</sub>, t, *J* = 6.1 Hz, 6H), 1.68–1.55 (propylCCH<sub>2</sub>C, s, 2H), 1.28–0.97 (OCH<sub>2</sub>CH<sub>3</sub>, s, 3H), and 0.61 (SiCH<sub>2</sub>, s, 2H). <sup>13</sup>C NMR (126 MHz, DMSO-*d*<sub>6</sub>) δ 160.10, 148.88, 144.58, 134.29, 133.93, 130.12, 129.35, 129.11, 128.66, 128.13, 125.76, 122.52, 118.94, 111.36, 110.53, 69.94, 64.15, 64.13, 59.72, 57.66, 21.49, 14.99, and 10.14. Calculated ESI-TOF-MS (*m/z*): 572 (M + H)<sup>+</sup> and observed mol. wt: 571.

#### X-Ray diffraction studies

The crystal of the complex 5c was mounted using Hampton cryoloops. All geometric and intensity data for the crystals were collected using a Super-Nova (Mo) X-ray diffractometer equipped with a micro-focus sealed X-ray tube Mo-Kα ( $\lambda = 0.71073$  Å) X-ray source, and an HyPix3000 detector with increasing  $\omega$  (width of 0.3 per frame) at a scan speed of either 5 or 10 s per frame. The CrysAlisPro software was used for data acquisition and data extraction. Using Olex2, the structure was solved with the SIR2004 structure solution program using direct methods and refined with the ShelXL refinement package using least squares minimization.<sup>31–33</sup> All non-hydrogen atoms were refined with anisotropic thermal parameters. Detailed crystallographic data and structural refinement parameters are summarized in Table 1. Bond angles and geometric parameters are listed in the ESI.†

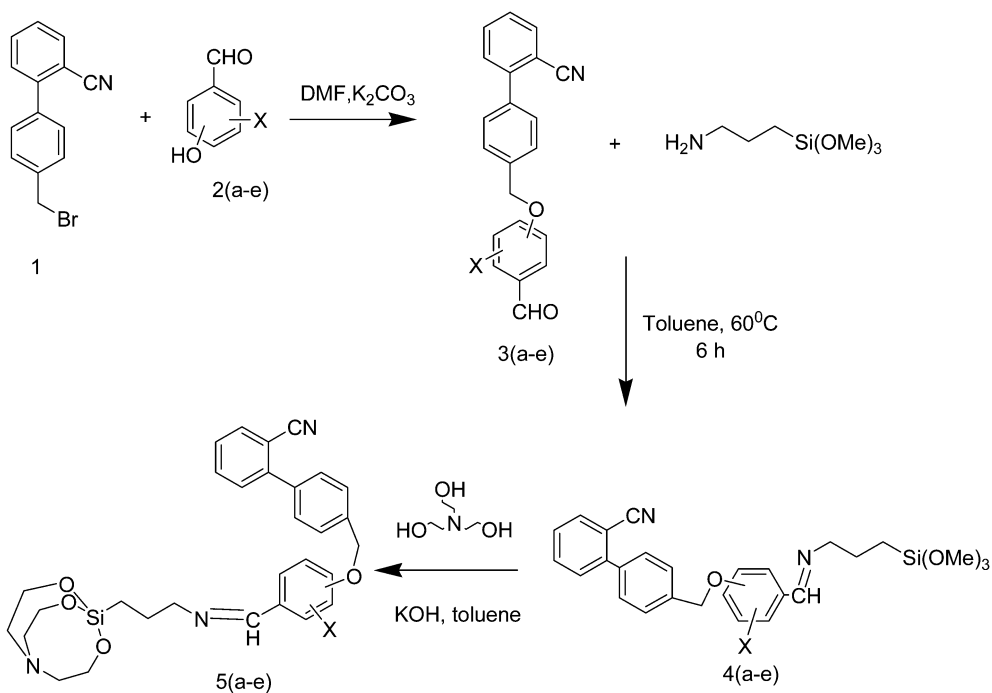
## Results and discussion

#### Synthesis and characterization

The synthetic route for the preparation of organosilatrane involves three steps and is shown in Scheme 1. In the first step, aryl alkyl ethers 3 (a–e) were synthesized by alkylation of hydroxybenzaldehydes 2(a–e) with 4-bromomethylbiphenyl-2-carbonitrile (2) under S<sub>N</sub>2 reaction conditions. The further condensation reaction between 3(a–e) and 2-aminopropylsilane gave organosilanes 4(a–e) and on

Table 1 Crystal data and structure refinement for 5c

Identification code	5c
Empirical formula	C <sub>30</sub> H <sub>32.5</sub> N <sub>3</sub> O <sub>4</sub> Si
Formula weight	527.18
Temperature/K	293(2)
Crystal system	Triclinic
Space group	<i>P</i> 1
<i>a</i> /Å	9.8540(5)
<i>b</i> /Å	12.4096(9)
<i>c</i> /Å	13.1516(6)
$\alpha$ /°	64.575(6)
$\beta$ /°	71.386(5)
$\gamma$ /°	85.694(5)
Volume/Å <sup>3</sup>	1372.88(16)
<i>Z</i>	2
$\rho_{\text{calc}}$ .g cm <sup>-3</sup>	1.275
$\mu$ /mm <sup>-1</sup>	0.126
<i>F</i> (000)	559.0
Crystal size/mm <sup>3</sup>	0.12 × 0.08 × 0.06
Radiation	Mo K $\alpha$ ( $\lambda$ = 0.71073)
2 $\theta$ range for data collection/°	6.48–54.868
Index ranges	–12 ≤ <i>h</i> ≤ 12, –15 ≤ <i>k</i> ≤ 15, –17 ≤ <i>l</i> ≤ 16
Reflections collected	19 002
Independent reflections	5863 [ <i>R</i> <sub>int</sub> = 0.0975, <i>R</i> <sub>sigma</sub> = 0.0790]
Data/restraints/parameters	5863/0/370
Goodness-of-fit on <i>F</i> <sup>2</sup>	1.100
Final <i>R</i> indexes [ <i>I</i> ≥ 2 $\sigma$ ( <i>I</i> )]	<i>R</i> <sub>1</sub> = 0.0713, <i>wR</i> <sub>2</sub> = 0.1893
Final <i>R</i> indexes [all data]	<i>R</i> <sub>1</sub> = 0.1104, <i>wR</i> <sub>2</sub> = 0.2352
Largest diffraction peak/hole/e Å <sup>-3</sup>	0.27/–0.38



a-X=H, o-OH, b- X=H, m-OH, c- X=H, p-OH, d- X=OCH<sub>3</sub>, o-OH, e- X=OCH<sub>2</sub>CH<sub>3</sub>, o-OH

Scheme 1 Synthesis of aryl-alkyl ether functionalized silatranes.

addition of triethanolamine along with a catalytic amount of potassium hydroxide to the organosilanes, in the final step, the desired organosilatranes **5(a-e)** were afforded. The structural

characterization of the obtained organosilatranes was performed to confirm their structure. <sup>1</sup>H NMR spectra exhibited signals at  $\delta$  = 0.5–0.65 ppm and  $\delta$  = 1.5–1.7 ppm corresponding to SiCH<sub>2</sub> and

CCH<sub>2</sub>C of the propyl chains in the synthesized compounds. Signals at 3.5–3.7 ppm and 5.20–5.30 ppm were also seen which can be assigned to OCH<sub>2</sub> and NCH<sub>2</sub> protons. A singlet was observed at

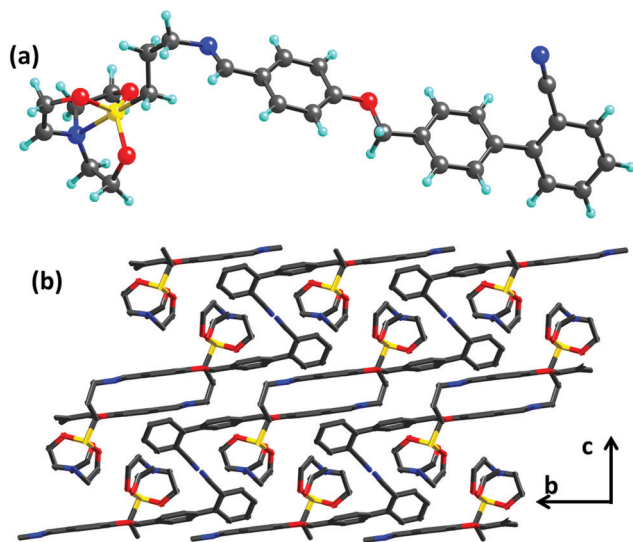


Fig. 1 (a) Ball and stick structures of compound **5c**. (b) The lattice arrangement of the compound **5c** along the *bc* plane.

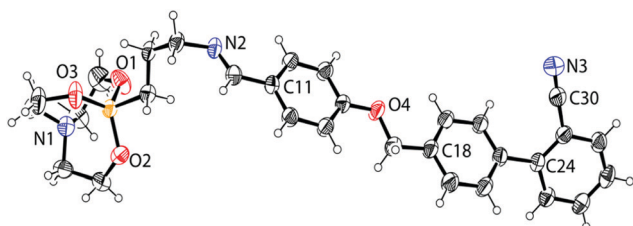


Fig. 2 ORTEP diagram of compound **5c** with a thermal ellipsoid at 40% probability. The disordered C-atoms of silatrane units were not shown for clarity.

8.2–8.5 ppm to confirm the formation of the Schiff base (HC=N). In organosilanes **4(a–e)**, the signal at 3.2–3.5 ppm confirmed the (OCH<sub>3</sub>)<sub>3</sub> group and in organosilatrane **5(a–e)**, the signals at 2.55–2.8 ppm and 3.4–3.6 ppm due to N(CH<sub>2</sub>)<sub>2</sub> and O(CH<sub>2</sub>)<sub>2</sub> authenticated the presence of the silatrane ring in the yielded compounds. <sup>13</sup>C NMR signals due to HC=N, N(CH<sub>2</sub>)<sub>2</sub>, O(CH<sub>2</sub>)<sub>2</sub> and OCH<sub>2</sub> in organosilatrane **5(a–e)** were observed in the range of 157–164 ppm, 48–50 ppm, 57–58 ppm and 69–70 ppm, respectively. The mass spectra of **5(a–e)** had base peaks at 528 (*M* + H<sup>+</sup>), 528 (*M* + H<sup>+</sup>), 528 (*M* + H<sup>+</sup>), 596 (*M* + K<sup>+</sup>), and 572 (*M* + H<sup>+</sup>), respectively, which further confirmed the structure of the prepared organosilatrane.

### X-Ray diffraction studies

Block shaped transparent single crystals of compound **5(c)** suitable for X-ray diffraction were grown by the slow evaporation of the mother liquor. The compound **5(c)** was crystallized in the triclinic crystal system with the *P* $\bar{1}$  space group. A labelled molecular view of the asymmetric unit of compound **5(c)** is shown in Fig. 1 and the ORTEP diagram is shown in Fig. 2. The structural elucidation confirms the aryl-alkyl ether moiety attached to the silatrane unit in a perpendicular manner, resulting in an L-shaped structure. The benzene units at both ends of the ether O-atoms have an almost planar arrangement, while the cyanosubstituted moiety is slightly off set from the rest of the units. There is no major H-bonding interaction within the molecules; however, there are a few weak interactions like C–H···N (3.20 Å) and C–H··· $\pi$  (3.78 Å) between silatrane (CH<sub>2</sub>) with cyano (N) and aryl benzene groups of the nearby units. In the lattice arrangement, all the silatrane heads are aligned in one line, while the aryl-alkyl tails are in the other line. The overall lattice arrangement of the compound **5(c)** results in a layer-like arrangement along the *bc* plane. The carbon atoms in the silatrane moiety were found to be disordered and the appropriate disordered model has been applied based on the available electron density.

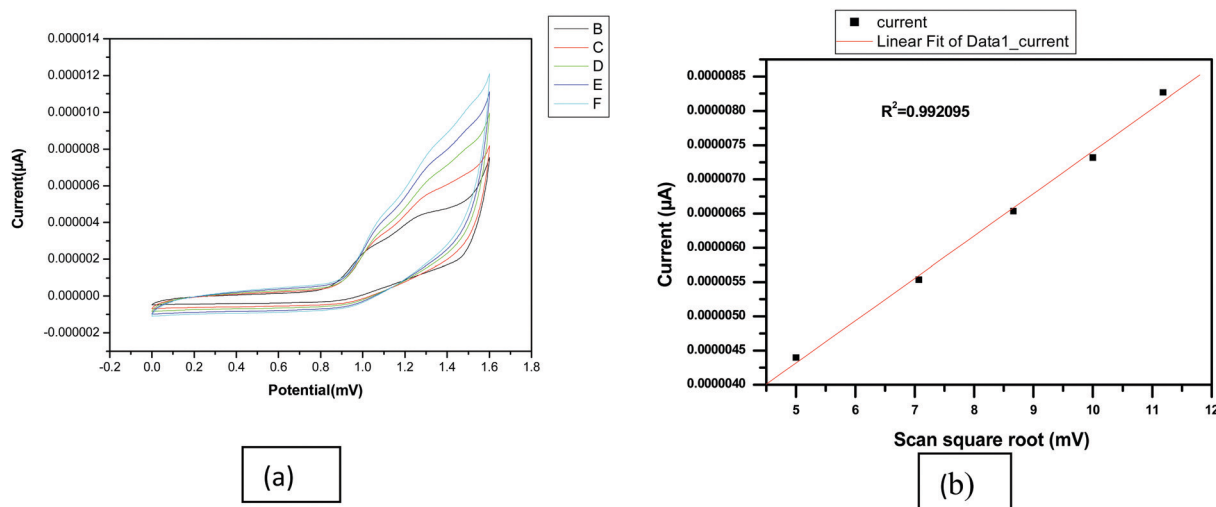


Fig. 3 (a) Scan rates at different potentials (mV) and (b) graph between current ( $\mu$ A) and square root of scan rate.

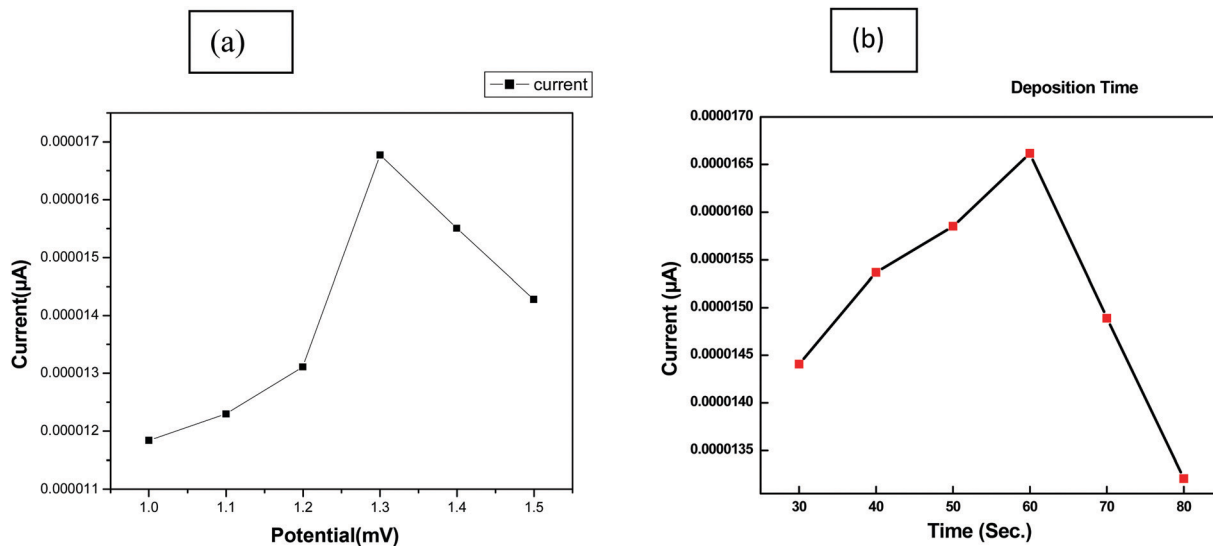


Fig. 4 Effect of (a) deposition potential and (b) deposition time on the voltammetric response of the sensor.

### Electrochemical studies

**Measurement procedure.** The gold electrode was polished by using  $\text{Al}_2\text{O}_3$  powder and rinsed with doubly distilled water between each polishing step. Then, it was washed with doubly distilled water successively and after drying properly, it was used for the experiment.

**Optimization of experimental parameters.** To obtain the maximum response of heavy metal ions, the different parameters such as deposition time and deposition potential influencing the response of  $\text{Al}^{3+}$  have been studied in methanol solvent using a gold electrode.

**Scan rate.** CV experiments were carried out at different scan rates from  $25 \text{ mV s}^{-1}$  to  $100 \text{ mV s}^{-1}$  and there was an electro-oxidation peak at a potential of 1.0 mV to 1.4 mV. The graph between current and square root of scan rate shows a linear response, which suggests a diffusional electrochemical process as shown in Fig. 3.

**Deposition potential and deposition time.** By holding the electrode at a fixed potential for some time, the effect of deposition potential from  $-1.5 \text{ V}$  to  $-1.0 \text{ V}$  was studied. With an increase in potential, the stripping current increases with the increase in the potential up to  $-1.3 \text{ V}$  and further increase in the potential (up to  $-1.0$ ) causes the current to decrease. So,  $-1.3 \text{ V}$  was chosen as the deposition potential for further analysis. By changing the time period from 30 s to 80 s, the effect of time was studied. The maximum current was observed at 60 s; after 60 s, the current is decreased up to 80 s, as shown in Fig. 4.

**Recognition studies.** The binding capacity of compound 5(e) with diverse metal cations such as  $\text{Co}^{2+}$ ,  $\text{Al}^{3+}$ ,  $\text{NH}_4^+$ ,  $\text{Ba}^{2+}$ ,  $\text{Ce}^{3+}$ ,  $\text{Ln}^{3+}$ ,  $\text{Hg}^{2+}$ ,  $\text{Ni}^{2+}$ ,  $\text{Sn}^{2+}$  and  $\text{Zn}^{2+}$  was examined by SWASV using a supporting electrolyte, a deposition potential of  $-1.3 \text{ V}$  and a deposition time of 60 s.<sup>34–36</sup> Among all the cations, the presence of the aluminium ion caused a shift in peak potential from  $-0.5 \text{ V}$  to  $-0.8 \text{ V}$ , while other cations do not show this nominal shift in the peak for current. This anomalous behaviour shows that the

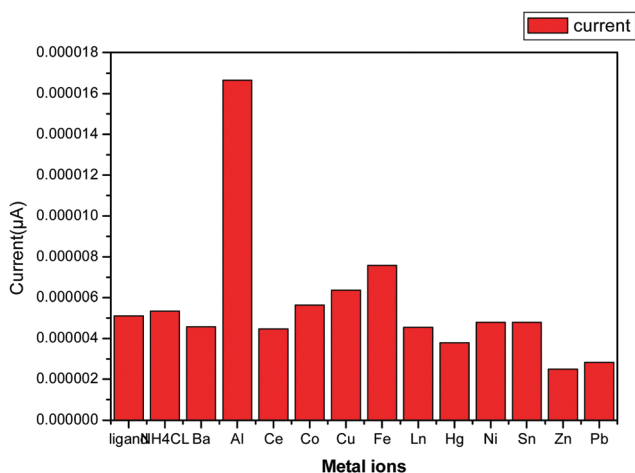


Fig. 5 Effect of different metal ions on the voltammetric response of the sensor.

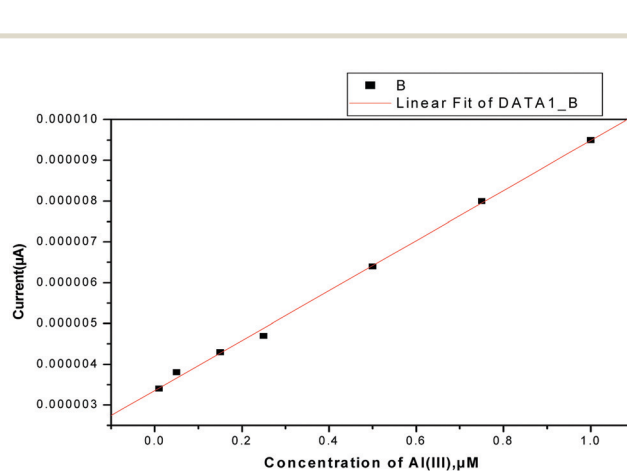


Fig. 6 Calibration plot for the detection of aluminium using different concentrations from  $0.01 \mu\text{M}$  to  $1 \mu\text{M}$  of  $\text{Al(III)}$ .

Table 2 Analysis of aluminium using different electrochemical techniques

Technique	Material	Linearity	LOD	Ref.
AdSV – adsorptive stripping voltammetry	Cupferon	240 s: 0.5–5 $\mu\text{g L}^{-1}$ , 120 s: 1–10 $\mu\text{g L}^{-1}$ , 60 s: 2–20 $\mu\text{g L}^{-1}$	0.5 $\mu\text{g L}^{-1}$	40
Stripping voltammetric	Aluminum–Alizarin S complex	5 to 45 $\mu\text{g L}^{-1}$	0.2 $\mu\text{g L}^{-1}$	41
AdCSV – adsorptive cathodic stripping voltammetry	Pyrogallol red	0–30 $\mu\text{g L}^{-1}$	1 $\mu\text{g L}^{-1}$	42
AdCSV – adsorptive cathodic stripping voltammetry	Portland cement	1–15 $\mu\text{g L}^{-1}$	0.11 $\mu\text{g L}^{-11}$	43
AdCSV – adsorptive cathodic stripping voltammetry	Al-1,2-dihydroxyanthraquinone-3-sulfonic acid (DASA)	0.8–30 $\mu\text{g L}^{-1}$	0.8 $\mu\text{g L}^{-1}$	44
Linear scan voltammetric	Norepinephrine	$4 \times 10^{-6}$ – $4 \times 10^{-5}$ mol L <sup>-1</sup>	$1.8 \times 10^{-6}$ mol L <sup>-1</sup>	45
Adsorptive cathodic stripping voltammetry	Al-8-hydroxyquinoline	$8.54 \times 10^{-8}$ to $2.35 \times 10^{-7}$ mol L <sup>-1</sup>	$8.54 \times 10^{-8}$ mol L <sup>-1</sup>	46
Stripping voltammetry	Solochrome violet RS complex	0–30 $\mu\text{g L}^{-1}$	0.15 $\mu\text{g L}^{-1}$	47

sensor has a special attraction towards Al(III) and the results are shown in Fig. 5.

**Linear response and limit of detection.** By changing the concentration of Al(III), the impact on the stripping current was considered.<sup>37–39</sup> A calibration bend was drawn between the metal concentration and the stripping current. A linear response of the current was observed in the range of 0.01–1  $\mu\text{M}$  for Al(III). After expanding the concentration of Al(III) up to 1.0  $\mu\text{M}$ , it was observed that the current was nearly consistent usually due to the saturation of metal ions on the electrode surface, and so no more Al(III) ions deposited on the active surface of the electrode (Fig. 6). The direct information was found from the data  $Y = 6.13387 \times 10^{-6} + 3.53389 \times 10^{-6}x$  ( $Y$ : peak current,  $\mu\text{A}$ , and  $x$ : concentration of Al(III),  $\mu\text{M}$ ) with a correlation coefficient of 0.99909. By using the  $3\sigma$  method, the limit of detection was calculated and it was found to be 48.9 nM, which paves the way for the use of organosilatrane as compared to

previous methods (Table 2). Fig. 7 shows the ion selectivity study where the effect of interference of other metal ions has been studied.

In the present situation, the synthesized organosilatrane contains a large number of donor locations and these donor sites are well furnished with lone pairs offering good covalent/non-covalent interactions with the target. So, the prepared sensor showed good selectivity towards the electrochemical detection of Al<sup>3+</sup> ions and poses the least interference from the other most probable interfering ions. The electrochemical performance was monitored using SWASV and excellent donor properties have also resulted in good detection limits.

**Real sample analysis.** This strategy was utilized to discover the concentration of Al(III) ions in tea leaves. Tea leaves were bought from a market and 1 g of the tea leaves was dissolved in 25 mL of methanol. The solution was stirred for 6 hours followed by centrifuging the mixture and then a methanol layer was separated out. The methanol layer was analysed by spiking with aluminium ions. The measure of aluminium was found to be exact indicating the negligible standard deviation (Table 3).

**Metal–aluminium complex.** To understand the binding mode, <sup>1</sup>H NMR titrations were carried out in both the absence and presence of Al(III) ions by utilizing different

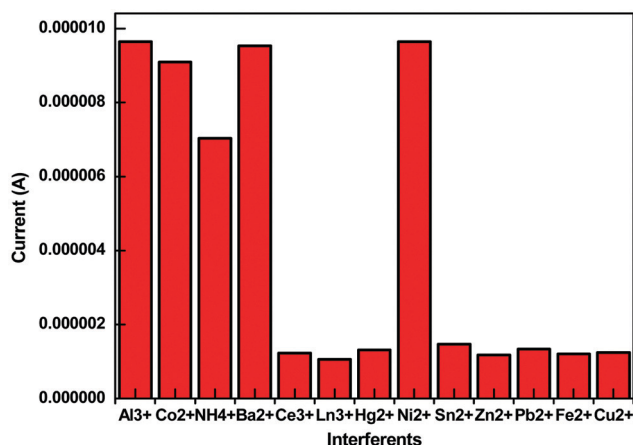
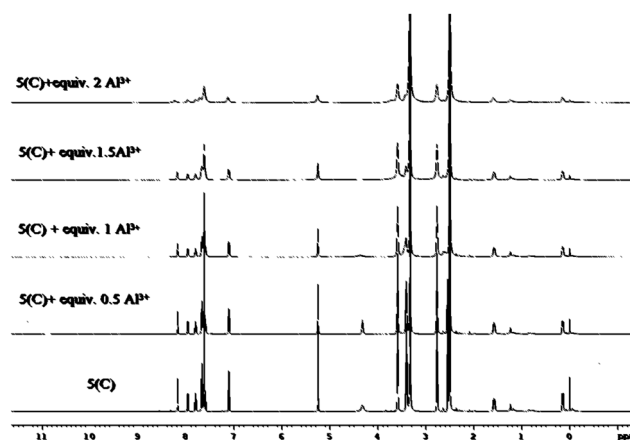


Fig. 7 Ion selectivity study.

Table 3 Determination of the Al(III) ions in real tea leaf samples

Tea leaves	Added $\mu\text{M}$	Found	Recovery (%)
	0.01	0.0099	99
	0.25	0.2487	99.4

Fig. 8 Effect on compound 5(C) on adding different equivalents of Al<sup>3+</sup> ions.

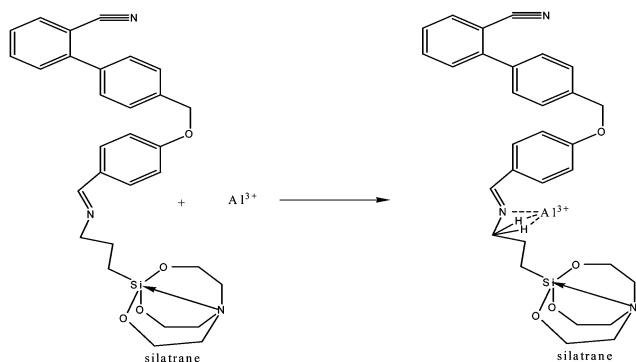


Fig. 9 Interaction of  $\text{Al}^{3+}$  ions with the receptor.

concentrations of  $\text{DMSO-}d_6$ . The impact of  $\text{Al(III)}$  can be observed as a broad peak of 2H at 4.2 ppm. On addition of 0.5 equivalent, a sharp peak of 2H was observed and after adding 1.0 and 1.5 equivalents, the intensity of the signal decreased. Finally, after addition of 2 equivalent of  $\text{Al(III)}$  ions, the intensity of the peak of 2H came out to be very small. It appears that the  $\text{Al(III)}$  interacts with the nitrogen atom and it impacts 2H present adjacent to the nitrogen atoms (Fig. 8). The plausible interaction of  $\text{Al}^{3+}$  ions with silatranes is shown in Fig. 9.

## Conclusions

In this article, we have synthesized aryl alkyl ether functionalized organosilatranes by using condensation and transesterification methodologies starting from 4-bromomethylbiphenyl-2-carbonitrile and hydroxybenzaldehydes. The prepared compounds were well characterized by different spectroscopic techniques and the structure of one of the obtained products was confirmed by X-ray crystallographic study. The prepared organosilatrane (5c) was utilized for a selective recognition study towards various metal cations using electrochemical analysis and the compound was found to show great affinity towards  $\text{Al}^{3+}$  ions. The  $\text{Al(III)}$  ions were determined electrochemically by differential pulse voltammetry techniques in the concentration range of 0.01–1  $\mu\text{M}$  with a limit of detection (LOD) value of 48.9 nm. The proposed chemosensors have also been used for the on-site detection of  $\text{Al(III)}$  ions in tea leaves. Furthermore, the interaction of  $\text{Al}^{3+}$  ions with organosilatranes was monitored using NMR by adding different equivalents of  $\text{Al}^{3+}$  ions. The spectroscopy study results suggest that the nitrogen of the imine group and the hydrogen of the adjacent methylene act as the potential binding site for the formation of complexes with the metals. Moreover, the sensing outcomes based on organosilatranes have been compared with the previously reported probes which pave the way for the use of the present work for the selective recognition of  $\text{Al(III)}$  ions.

## Conflicts of interest

There are no conflicts of interest.

## Acknowledgements

The authors are grateful to CSIR and DST-PURSE for providing financial assistance.

## References

- 1 J. G. Verkade, *Acc. Chem. Res.*, 1993, **26**, 483.
- 2 R. Zitz, J. Baumgartner and C. Marschner, *Organometallics*, 2019, **38**, 1159.
- 3 G. Singh, Priyanka, A. Singh, P. Satija, Sushma, Pawan, Mohit, J. Singh and J. Singh, *New J. Chem.*, 2021, **45**, 7850.
- 4 G. Singh, G. Kaur and J. Singh, *Inorg. Chem. Commun.*, 2018, **88**, 11.
- 5 A. B. Trofimov, V. G. Zakrzewski, O. Dolgounitcheva, J. V. Ortiz, V. F. Sidorkin, E. F. Belogolova, M. Belogolov and V. A. Pestunovich, *J. Am. Chem. Soc.*, 2005, **127**, 986.
- 6 S. Durdagi, B. Aksoydan, I. Erol, I. Kantarcioglu, Y. Ergun, G. Bulut, M. Acar, T. Avsar, G. Liapakis, V. Karageorgos and R. E. Salmas, *Eur. J. Med. Chem.*, 2018, **145**, 273.
- 7 G. Singh and S. Rani, *Sens. Actuators, B*, 2017, **244**, 861.
- 8 Sudheer, V. Kumar, P. Kumar and R. Gupta, *New J. Chem.*, 2020, **44**, 13285.
- 9 N. A. Eltahawy, O. M. Sarhan, A. S. Hammad and S. Abu-nour, *J. Radiat. Res. Appl. Sci.*, 2016, **9**, 400.
- 10 N. V. Gorantla, V. G. Landge, P. G. Nagaraju, P. Priyadarshini, E. Balaraman and S. Chinnathambi, *ACS Omega*, 2019, **4**, 16702.
- 11 A. Kumar, R. Pandey, A. Kumar and D. S. Pandey, *RSC Adv.*, 2014, **4**, 55967.
- 12 A. Roth, C. Nogues, P. Galle and T. Druke, *Virchows Arch. A: Pathol. Anat. Histopathol.*, 1984, **405**, 131.
- 13 H. Nakamura, P. G. Rose, J. L. Blumer and M. D. Reed, *J. Clin. Pharmacol.*, 2000, **40**, 296.
- 14 J. Fu, Y. Chang, B. Li, X. Wang, X. Xie and K. Xu, *Spectrochim. Acta, Part A*, 2020, **225**, 117493.
- 15 K. Sato, I. Suzuki, H. Kubota, N. Furusho, T. Inoue, Y. Yasukouchi and H. Akiyama, *Food Sci. Nutr.*, 2014, **2**, 389.
- 16 F. Ahmadi and A. A. Alizadeh, *J. Neurol. Sci.*, 2017, **381**, 313.
- 17 M. R. Awual and M. M. Hasan, *J. Mol. Liq.*, 2019, **294**, 111679.
- 18 M. R. Awual, T. Yaita, T. Kobayashi, H. Shiwaku and S. Suzuki, *J. Environ. Chem. Eng.*, 2020, **8**, 103684.
- 19 M. R. Awual, M. M. Hasan, A. Islam, A. M. Asiri and M. M. Rahman, *J. Mol. Liq.*, 2020, **298**, 112035.
- 20 M. R. Awual, M. M. Hasan, A. M. Asiri and M. M. Rahman, *J. Mol. Liq.*, 2019, **283**, 704.
- 21 M. R. Awual, M. M. Hasan, A. Islam, M. M. Rahman, A. M. Asiri, M. A. Khaleque and M. C. Sheikh, *J. Cleaner Prod.*, 2019, **228**, 778.
- 22 M. M. Alam, A. M. Asiri, M. T. Uddin, M. A. Islam, M. R. Awual and M. M. Rahman, *New J. Chem.*, 2019, **43**, 4849.
- 23 T. A. Sheikh, M. N. Arshad, M. M. Rahman, A. M. Asiri, H. M. Marwani, M. R. Awual and W. A. Bawazir, *Inorg. Chim. Acta*, 2017, **464**, 157.
- 24 A. Shahat, H. M. Hassan, M. F. El-Shahat, O. El Shahawy and M. R. Awual, *Chem. Eng. J.*, 2018, **334**, 957.

- 25 M. M. Alam, A. M. Asiri, M. T. Uddin, M. A. Islam, M. R. Awual and M. M. Rahman, *New J. Chem.*, 2019, **43**, 8651.
- 26 T. A. Sheikh, M. M. Rahman, A. M. Asiri, H. M. Marwani and M. R. Awual, *J. Ind. Eng. Chem.*, 2018, **66**, 446.
- 27 M. R. Awual, M. M. Hasan, J. Iqbal, M. A. Islam, A. Islam, S. Khandaker, A. M. Asiri and M. M. Rahman, *J. Environ. Chem. Eng.*, 2020, **8**, 103591.
- 28 M. R. Awual, M. M. Hasan, J. Iqbal, A. Islam, M. A. Islam, A. M. Asiri and M. M. Rahman, *Microchem. J.*, 2020, **154**, 104585.
- 29 A. I. Vogel, *A textbook of Practical Organic Chemistry*, Logman, London, 4th edn, 1978.
- 30 S. Hidalgo-Figueroa, J. J. Ramírez-Espinosa, S. Estrada-Soto, J. C. Almanza-Pérez, R. Román-Ramos, F. J. Alarcón-Aguilar, J. V. Hernández-Rosado, H. Moreno-Díaz, D. Díaz-Coutiño and G. Navarrete-Vazquez, *Chem. Biol. Drug Des.*, 2013, **81**, 474.
- 31 O. V. Dolomanov, L. J. Bourhis, R. J. Gildea, J. A. K. Howard and H. Puschmann, *J. Appl. Crystallogr.*, 2009, **42**, 339.
- 32 M. C. Burla, R. Caliendo, M. Camalli, B. Carrozzini, G. L. Cascarano, L. De Caro, C. Giacovazzo, G. Polidori, D. Siliqi and R. Spagna, *J. Appl. Crystallogr.*, 2007, **40**, 609.
- 33 G. Sheldrick, *Acta Crystallogr., Sect. C: Struct. Chem.*, 2015, **71**, 3.
- 34 M. M. Rahman, M. M. Hussain, M. N. Arshad, M. R. Awual and A. M. Asiri, *New J. Chem.*, 2019, **43**, 9066.
- 35 M. M. Rahman, T. A. Sheikh, A. M. Asiri and M. R. Awual, *New J. Chem.*, 2019, **43**, 4620.
- 36 S. Khandaker, Y. Toyohara, G. C. Saha, M. R. Awual and T. Kuba, *J. Water Process Eng.*, 2020, **33**, 101055.
- 37 A. Islam, S. H. Teo, M. R. Awual and Y. H. Taufiq-Yap, *J. Cleaner Prod.*, 2019, **238**, 117887.
- 38 R. M. Kamel, A. Shahat, W. H. Hegazy, E. M. Khodier and M. R. Awual, *J. Mol. Liq.*, 2019, **285**, 20.
- 39 A. Islam, T. Ahmed, M. R. Awual, A. Rahman, M. Sultana, A. A. Aziz, M. U. Monir, S. H. Teo and M. Hasan, *J. Cleaner Prod.*, 2020, **244**, 118815.
- 40 G. Kefala, A. Economou and M. Sofoniou, *Talanta*, 2006, **68**, 1013.
- 41 J. Zuziak and M. Jakubowska, *J. Electroanal. Chem.*, 2017, **794**, 49.
- 42 V. Arancibia and C. Munoz, *Talanta*, 2017, **73**, 546.
- 43 N. A. El-Maali, Y. M. Temerk and M. S. El-Aziz, *Anal. Chim. Acta*, 1997, **353**, 313.
- 44 L. M. de Carvalho, P. C. do Nascimento, D. Bohrer, R. Stefanello and D. Bertagnolli, *Anal. Chim. Acta*, 2005, **546**, 79.
- 45 F. Zhang, M. Ji, Q. Xu, L. Yang and S. Bi, *J. Inorg. Biochem.*, 2005, **99**, 1756.
- 46 L. B. Santos, M. T. de Souza, A. T. Paulino, E. E. Garcia, E. M. Nogami, J. C. Garcia and N. E. de Souza, *Microchem. J.*, 2014, **112**, 50.
- 47 J. Wang, P. A. Farias and J. S. Mahmoud, *Anal. Chim. Acta*, 1985, **172**, 57.